Computational Evaluation of the Effect of Build Orientation on Thermal Behavior and in-situ Martensite Decomposition for Laser Powder-Bed Fusion (LPBF) Process

Ayse Kubra YILDIZ[*] iD , Mehmet MOLLAMAHMUTOGLU iD , Oguzhan YILMAZ iD

Advanced Manufacturing Technologies Research Group (AMTRG), Department of Mechanical Engineering, Faculty of Engineering, Gazi University, Maltepe, 06570, Ankara, Turkey

Highlights
• This paper focuses on the effect of different build orientations.
• An effective model was designed for laser powder bed fusion.
• The effect of build orientation on martensite decomposition is emphasized.

Abstract

Laser powder bed fusion (LPBF), which is an additive manufacturing method, is a thermo-mechanical process in which instantaneously varying heat flow rates occur by moving a high-intensity laser beam. The high temperatures and cooling rates that occur throughout the process result in microstructures with brittle behavior. The microstructure and mechanical properties may be improved by controlling the cooling rates in the layers via build orientation. Since the process is on a microscale, it requires planning as it does not allow instant intervention. Therefore, numerical analysis can be helpful to determine the effect of different build orientations. In this study, the effect of different build orientations was emphasized. For this purpose, successive layers resulting in narrowing and expanding cross-sectional areas were investigated with a detailed thermal approach. Also, a martensite decomposition case, as a result of changing the build orientation for a geometry, was presented numerically. As a result, it is shown that build orientation has an effect on the heat distribution within the part. Some benefits of expanding the cross-sectional area have been determined. Specifically, it is found that the build orientation may also enable local martensite decomposition, contributing to a lamellar microstructure.

1. INTRODUCTION

Laser powder-bed fusion (LPBF) is one of the additive manufacturing emerging in the 1990s and continues to be developed today [1,2]. This method is the melting of metal powders laid in a shielding gas environment by scanning with a high-energy laser beam, then the process is repeated by lowering the bottom plate one layer. LPBF, which has advantages such as rapid and mass production of specific and complex geometries without wasting material, is widely used in the automotive, biomedical and energy industries, especially in aerospace and aviation. Popular for its advantages, LPBF is expected to meet the necessities of mechanical quality standards for the final product. For this reason, studies on improving the mechanical and microstructural properties of LPBF parts are still ongoing. In this context, variations in process parameters are known to significantly affect the microstructure and mechanical properties (strength, density, surface quality, etc.) of the final part [3].

The build orientation is one of the issues that should be paid attention to in terms of part quality. It can obtain various microstructure and mechanical properties by producing the same geometry parts with different structural angles and directions [4]. Previous studies in the literature have mostly focused on horizontal-vertical directions and some off-axis performance, and these studies have experimentally demonstrated the effect of orientation on strength, ductility, fatigue, porosity, surface quality, and residual

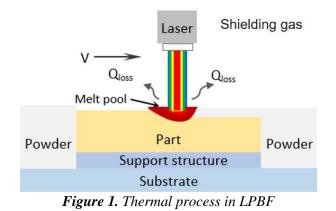*Corresponding author, e-mail: aysekubra.yildiz@gazi.edu.tr*

stress [5,6]. Uncertainty remains about how build orientation affects mechanical properties. These effects are complex and are radically based on many thermo-mechanical events occurring in the process. Experimentally, it is very difficult to measure rapidly changing heat flow rates at the microscale in LPBF. Therefore, numerical studies are required for the thermal effects of build orientation.

Ti6Al4V alloy is widely preferred in LPBF applications due to its superior material properties. Ti6Al4V consists of pure Ti alloyed with 6% Al (α stabilizer) and 4% V (β stabilizer) by weight. It is possible to obtain various microstructures as a result of different thermal applications. Depending on the cooling rate, different phases (α',α) may occur in the Ti6Al4V alloy, which reaches high temperatures with thermal processes. [7,8]. Low and medium cooling rates cause α-lamellar phases to nucleate and grow through the β grains, while the β phase completely transforms into the α' martensitic phase at high cooling rates [9,10]. In addition, it is possible to form two-phase (α+β) lamella structures or equiaxed structures [7]. Due to rapid cooling during solidification, acicular martensite α' structure with high hardness is formed in the parts produced with LPBF. This microstructure shows high strength but low ductility and toughness [11]. In most circumstances, it is undesirable in terms of engineering quality standards. On the other hand, higher strength and ductility can be obtained by α+β microstructure. The in-situ decomposition method, which is focused on heat storage and cooling rate control approaches in the layer, enables the transformation of α' martensite into α+β microstructures without post-processing [12, 13]. There has not been any study yet on the effect of build orientation on martensite decomposition. Thus, an effective model was designed to explain the possible thermal effects of build orientation. Detailed thermal analyzes were performed for structures with narrowing and expanding cross-sectional areas in each new layer. In addition, how different build orientations may affect martensite decomposition was evaluated computationally for a geometry.

2. MATERIALS AND METHODS

2.1. Thermophysical Phenomena

In LPBF, the upper surface of the metal powders laid in a protective gas environment is scanned by the laser. During scanning, some of the laser energy is lost on the upper surface of the layer due to reflection, evaporation, convection and radiation, while the rest is penetrated through the material by conduction. The metal powders melted by the absorbed energy form a molten pool on a microscale (Figure 1). Thus, the layers experience a series of transformations from powder to liquid and finally solid phases.

Figure 1. Thermal process in LPBF

In LPBF, the parts are produced in a powder bed, which has a very low conductivity due to the gaps between powders (Table 1). Therefore, most of the absorbed heat flows through the solidified layers towards the substrate. Using this feature, the microstructure and mechanical property can be improved by controlling the heat accumulation and cooling rate in the layers with build orientation. Narrowing in the direction of heat flow can help increase the temperature stored in the layers (Figure 2). Thus, it can also help in providing the special conditions required for martensite decomposition.
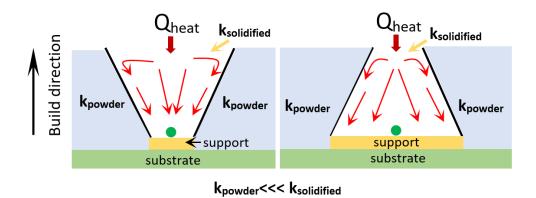
Figure 2. *The heat conduction within the part in different orientations in LPBF*

2.2. Governing Equations, Material Properties and Parameters

The model was designed as multi-track and multi-layer compatible with reality. General heat transfer equation of L-PBF is below:

$$\rho c \frac{\partial T}{\partial t} = \frac{\partial}{\partial x}\left(k\frac{\partial T}{\partial x}\right) + \frac{\partial}{\partial y}\left(k\frac{\partial T}{\partial y}\right) + \frac{\partial}{\partial z}\left(k\frac{\partial T}{\partial z}\right) + Q. \tag{1}$$

Here, ρ, c, T, k and Q are the density (kg/m^3), the specific heat capacity (J/kgK), the temperature, the thermal conductivity (W/mK) and volumetric heat input/output (W/m^3), respectively. The laser heat source is defined as a Gaussian distribution on the upper surface of the layer,

$$q = \frac{2\tau P}{\pi r^2}\exp\left(-\frac{2(x^2+y^2)}{r^2}\right) \tag{2}$$

q, τ, P and r are the heat flux, the absorptivity, the power and the laser beam radius, respectively.

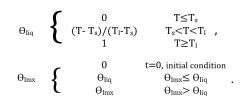The ambient temperature (T_0) has been defined as the initial condition (t = 0) for the entire domain

$$T\,(x, y, z, t)\,|_{t=0} = T_0 \tag{3}$$

Convection and radiation losses are defined on the upper surface (Equation (4)) (In all other domain boundaries, a constant temperature condition is defined at a suitable distance)

$$Q_{conv} = h_c(T - T_0), \tag{4}$$
$$Q_{rad} = \sigma\varepsilon(T^4 - T_0^4).$$

In the process, it can be thought that some of the powder first turns into liquid and then into the bulk material (densified solid). Thus, hysteresis material behavior is defined to strengthen the model, and phase fractions (Θ_{liq} and Θ_{lmx}, Equation (5)) were added to the domain

$$\theta_{liq} \begin{cases} 0 & T \leq T_s \\ (T-T_s)/(T_l-T_s) & T_s < T < T_l \\ 1 & T \geq T_l \end{cases},$$

$$\theta_{lmx} \begin{cases} 0 & t=0, \text{ initial condition} \\ \theta_{liq} & \theta_{lmx} \leq \theta_{liq} \\ \theta_{lmx} & \theta_{lmx} > \theta_{liq} \end{cases}. \tag{5}$$

Here, T_s is the solidus temperature (1877 K) and T_l is the liquidus temperature (1923 K) [14]. Therefore, phase transformations (powder→liquid→solid) were performed, and their phase histories were consistently updated and maintained during simulation. The thermophysical properties of Ti6Al4V are temperature dependent, and the graph derived from previous studies [15,16] for the thermal conductivity and specific heat capacity properties is shown in Figure 3. In addition, the latent heat of fusion (L) and density (ρ) for this alloy was defined as 286 kJ/kg and 4200 kg/m^3, respectively [17]. The temperature-dependent emissivity data were taken from previous studies [18]. In the model, the solid properties of Ti6Al4V were assigned to the substrate and support structure.
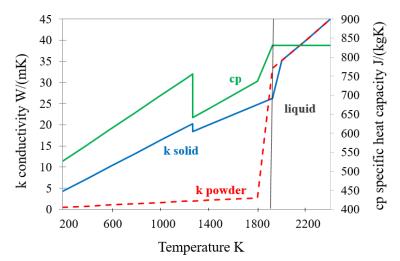

Figure 3. Thermal conductivity and specific heat capacity properties for Ti6Al4V

After reviewing the previous studies and trial-error procedure, a suitable parameter combination was determined. The parameter values are shown in Table 1. Numerous thermophysical phenomena occur in laser-powder interactions. All these phenomena greatly complicate the process and lead to very high computational costs. On the other hand, taking these phenomena into account increases the accuracy and authenticity of the numerical results. Therefore, an efficient absorptivity expression is used in the model for highly complex and time-consuming laser powder bed processes. It has been determined that there is no need to increase the anisotropic enhanced factors, which might be needed as a result of the recoil pressure and the Marangoni effect for the parameter set. The powder layer has a porosity structure, and after solidification, the layer thickness decrease with the effect of the collapse depending on the relative powder density. There are approaches to this issue in the literature [19, 20], and one of them is the calculation of effective solidified layer thicknesses for each layer [20]. Therefore, in this study, effective solidified layer thicknesses for each layer were calculated and defined by using the effective thickness expression [20].

Table 1. Process parameters used

Parameter	Value
Power [W]	375
Laser speed [mm/s]	1000
Laser diameter [μm]	180
Powder layer porosity [-]	0.5 [21]
Nominal powder layer thickness [μm]	60

Effective solidified layer thickness [µm]	30→60
Hatch distance [µm]	120
Initial and substrate temperature [K]	473
Absorptivity [-]	0.4 [22]
Anisotropic enhanced factors in z direction [-]	$\lambda_z=1$
Convective heat transfer coefficient [W/m²K]	10 [23]
Inter-layer time, powder laying time (cooling time) [s]	1
Support thickness [mm]	2
Support void ratio [%]	75
Support void conductivity factor [-]	0.1[22]

2.3. Modelling of Narrowing and Expanding Cross-sectional Areas in the Build Direction

In this study, to determine the effect of build orientation, the thermal results in the layers were analyzed by numerically modeling two parts with the same geometry, expanding and narrowing in one axis in the build direction. The scanned area of the expanding orientation increases (5→13 tracks) in 5 layers, while the scanned area of the narrowing orientation decreases (13→5 tracks) in 5 layers, and the same part is produced in total (Figure 4). For simplicity, the results of the P point in the center on the first layer are shown, representing the entire layer.
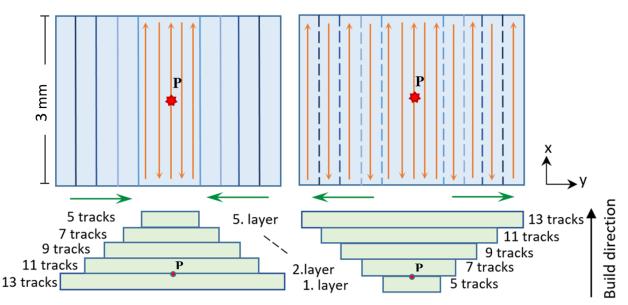

Figure 4. *The build orientation of narrowing (a) and expanding (b) parts*

The developed model was generated in the Comsol Multiphysics program. The domain was meshed with 13000 elements for two separate cases (Figure 5). The scanned area is meshed with a much finer mesh, as it experiences instantaneous thermo-mechanical changes at the micro scale.
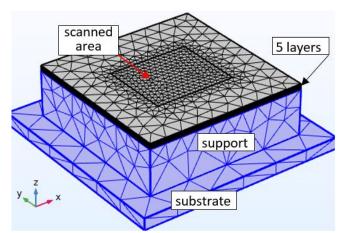
***Figure 5.** The mesh geometry for narrowing and expanding parts*

2.4. Modeling of a Geometry for Martensite Decomposition

The positive effect of martensite decomposition on microstructure and mechanical performance is known [12, 13], and in this context, the effect of build orientation on decomposition was evaluated. In this study, two parts with the same geometry were designed in 12 layers. One of these parts is expanding-constant (EC) oriented and the other is constant-narrowing (CN) oriented (Figure 6). The domain was meshed with 25000 elements for two separate cases. By calculating the layer-by-layer temperature histories of these parts, the effect of their orientation on possible martensite decomposition was compared.
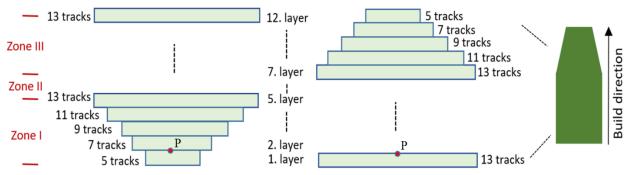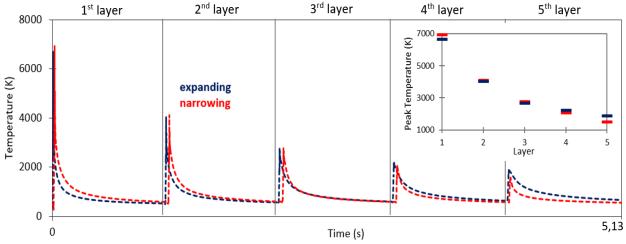

***Figure 6.** The build orientation of expanding-constant (a) and constant-narrowing (b) parts*
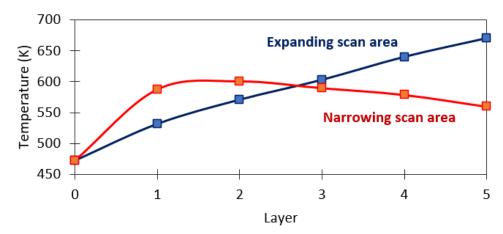
3. RESULTS AND DISCUSSION

3.1. Thermal Structure of Narrowing and Expanding Cross-sectional Areas in the Build Direction

As the five subsequent layers (expanding and narrowing) are scanned, the detailed thermal history of the P point on the 1st layer is presented in Figure 7. Approximately, a total of 6 hours were calculated for two separate events with 5 layers. Adjacent tracks and subsequent layers scanned hierarchically affect the temperature of the P point in proportion to the distance. As the distance of the scanned layers to the P point increases, the jump in temperature at the P point is decreased. Due to the narrowing's higher tracks at first, the maximum temperatures of the narrowing are higher than the expanding. But then, the maximum temperatures of the expanding exceed the narrowing with the addition of layers owing to the expanding's increasing tracks (Figure 7).

Figure 7. *The temperature of P point on the 1st layer during scanning of 5 subsequent layers for narrowing and expanding parts*

The layer is affected by thermal cycles (heating-cooling) occurring in the subsequent layers. This effect increases the temperature of the deposited layer for a while as the subsequent layers are added, forming a kind of thermal bridge. The temperatures stored in 1st layer for the shrinking(a) and expanding (b) parts are shown in Figure 8. Thanks to the continuous increase in the scanning area for the expanding part, the total energy applied to the layer rises, and the temperature stored at point P is constantly increasing. On the other hand, the narrowing part has higher temperatures stored at first due to the higher scanning area. But, owing to the continuous decrease in the scanning area for each new layer, the total energy applied to the layer decreases, and the temperature stored is constantly decreasing. Thus, comparing different orientations of the same geometry, it has been determined that the temperatures stored in the layers are different, and the expanding build direction (the reverse of heat flow) is more beneficial in terms of temperature storage. The contraction in the direction of the heat flow causes the temperature increase in the lower layers.

Figure 8. *The temperature stored on 1st layer during scanning of 5 layers for narrowing and expanding parts*

3.2. The Effect of Different Orientations in a Geometry on Martensite Decomposition

The temperatures stored in the 1st layer of the 12-layered two parts modeled to examine the effect of build orientation on martensite decomposition are as in Figure 9. Approximately, a total of 30 hours were calculated for two separate cases with 12 layers. These parts have seven layers with constant scan area and five layers with expanding or narrowing scan area (same geometries in total). In zone, I (first five layers), the scan area of CN is constant (13 tracks) while the scan area of EC increases (5→13 tracks) for each new layer. As a result of scanning five layers, they reached almost the same temperature stored. In zone II,

similar temperature results were calculated as the same scanning area was continued for both cases. Finally, since the scan area of CN decreases (13→5 tracks) for each new layer in zone III (last five layers), the temperature stored is decreased gradually. However, the scan area of EC is constant (13 tracks), and the temperature stored is stable.
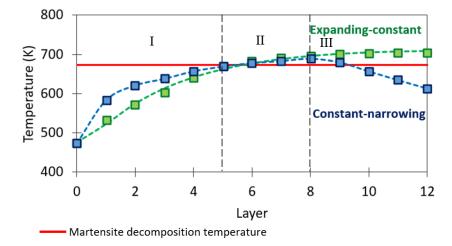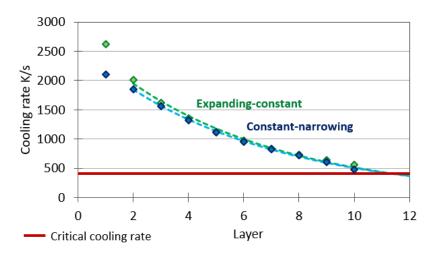

Figure 9. *The temperature stored on 1st layer during scanning of 12 layers for expanding-constant and constant-narrowing parts*

Certain conditions need to be met for martensite decomposition to occur. The first of these conditions is that the temperature of the deposited layer needs to be kept above the initiation temperature of the martensite decomposition (Tmd, 400°C, 673 K for Ti6Al4V alloy) for a sufficiently long time [24]. The second is that it is necessary to decrease the cooling rate below the critical cooling rate, which is 410 K/s for the decomposition in Ti6Al4V [25].

Despite having the same geometry, the 1st layer of the part with CN build orientation remained above the Tmd temperature for a little time (insufficient for decomposition), while the 1st layer of the part with EC build orientation remained for a long time. Furthermore, during the time the temperature stored remained above the Tmd temperature in CN build orientation, decomposition could not occur because the cooling rate was over 410 K/s (Figure 10). In EC build orientation, the cooling rate decreased below 410 K/s following ten layers. At the same time, the Tvs temperature remained above the Tmd temperature. Since two conditions were met, decomposition could begin in EC.

Figure 10. *The cooling rate of 1st layer during scanning of 12 layers for expanding-constant and constant-narrowing parts*

In this study, the build orientation case was examined conceptually in the context of heat transfer. Therefore, the expanding part is designed in such a way that the support structure is not needed [26] (with higher than 45° of building angle and less layers). On the other hand, support structures may be needed in case of an angle less than 45 degrees and deterioration in the expanding parts. In this case, conductivity may increase slightly due to the support structure. In addition, inter layer time may also increase due to building time of support in each layer. In this way, it will be useful to investigate the effect of various support structures (geometry, porosity etc.) in complex expanding parts in future studies.

4. CONCLUSIONS

Various microstructure and mechanical properties can be acquired by producing the same geometry parts with different structural angles and directions. Since the build orientation can control the heat transfer within the part, it can play a helpful role in obtaining some desired mechanical properties.

In this study, the effects of the build orientation in LPBF are shown by thermal analysis of the same geometry in different orientations. It has been observed that the build orientation plays a role in determining the thermal history and cooling rates of the layers, and the expanding build direction (the reverse of heat flow) is more beneficial. It has also been shown that the build orientation can enable martensite decomposition in some sections and assist in obtaining a lamellar microstructure.

In order to clearly show the effects of the build oration on thermal history and cooling rates, this study focused on a basic build orientation (changing in one axes). In future studies, it is considered that it will be useful to investigate and develop this subject in complicated parts in various build orientations.

CONFLICTS OF INTEREST

No conflict of interest was declared by the authors.

REFERENCES

[1] Eshawish, N., Malinov, S., Sha, W., Walls., P., "Microstructure and mechanical properties of Ti-6Al-4V manufactured by selective laser melting after stress relieving, hot isostatic pressing treatment, and post-heat treatment", Journal of Materials Engineering and Performance, 30, 5290–5296, (2021).

[2] Taylor, H.C., Garibay, E.A., Wicker, R.B., "Toward a common laser powder bed fusion qualification test artifact", Additive Manufacturing, 39, 101803, (2020).

[3] Kruth, J.P., Badrossamay, M., Yasa, E., Deckers, J., Thijs, L., Humbeeck, J. "Part and material properties in selective laser melting of metals", 16th International Symposium on Electromachining, ISEM 2010, (2010).

[4] Mfusi, B.J., Tshabalala, L.C., Popoola, A.P.I., Mathe, N.R., "The effect of selective laser melting build orientation on the mechanical properties of AlSi10Mg parts", 2018 IOP Conference Series Materials Science and Engineering, 430, 012028, (2018).

[5] Ren, S., Chen, Y., Liu, T., Qu, X., "Effect of Build Orientation on Mechanical Properties and Microstructure of Ti-6Al-4V Manufactured by Selective Laser Melting", Metallurgical and Materials Transactions A, 50, 4388–4409, (2019).

[6] Alsalla, H.H., Smith, C., Hao, L., "Effect of build orientation on the surface quality, microstructure and mechanical properties of selective laser melting 316L stainless steel", Rapid Prototyping Journal, 24(1): 9-17, (2018).

[7] Welsch, G., Boyer, R., Collings, E., "Materials properties handbook: titanium alloys", ASM international, (1993).

[8] Kim, H.Y., Miyazaki, S., "Martensitic transformation and superelastic properties of Ti-Nb base alloys", Materials Transactions, 56, 625-634, (2015).

[9] Zhang, X., Yocom, C.J., Mao, B., Liao, Y., "Microstructure evolution during selective laser melting of metallic materials: A review", Journal of Laser Applications, 31, 031201, (2019).

[10] Filip, R., Kubiak, K., Ziaja, W., Sieniawski, J., "The effect of microstructure on the mechanical properties of two-phase titanium alloys", Journal of Materials Processing Technology, 133, 84–89, (2003).

[11] Xu, W., Sun, S., Elambasseril, J., Liu, Q., Brandt, M., Qian, M., "Ti-6Al-4V additively manufactured by selective laser melting with superior mechanical properties", The Minerals, Metals & Materials Society, (2015).

[12] Xu, W., Brandt, M., Sun, S., Elambasseril, J., Liu, Q., Latham, K., Xiad, K., Qian, M., "Additive manufacturing of strong and ductile Ti–6Al–4V by selective laser melting via in situ martensite decomposition", Acta Materialia, 85, 74–84, (2015).

[13] Xu, W., Lui, E.W., Pateras, A., Qjan, M., Brandt, M., "In situ tailoring microstructure in additively manufactured Ti-6Al-4V for superior mechanical performance", Acta Materialia, 125, 390-400, (2017).

[14] Boyer, R, Welsch, G., Collings, E.W., "Materials properties handbook: titanium alloys", ASM International, ISBN 978-0871704818, Materials Park, OH, (1994).

[15] Mills, K.C., "Recommended values of thermophysical properties for selected commercial alloys", first ed., Woodhead Publishing Ltd, (2002).

[16] Gong, X., Cheng, B., Price, S., Chou, K., "Powder-bed electron-beam-melting additive manufacturing: powder characterization, process simulation and metrology", ASME Early Career Technical Conference (ECTC), District F, 59-66, (2013).

[17] Fan, Z., Liou, F., "Numerical modeling of the additive manufacturing (am) processes of titanium alloy. in: titanium alloys-towards achieving enhanced properties for diversified applications", first edition, IntechOpen, (2012).

[18] Parry, L., Ashcroft, I.A.R., Wildman, D., "Understanding the effect of laser scan strategy on residual stress in selective laser melting through thermo-mechanical simulation", Additive Manufacturing, 12, 1-15, (2016).

[19] Riedlbauer, D., Scharowsky, T., Singer, R.F., Steinmann, P., Körner, C., Mergheim, J., "Macroscopic Simulation and Experimental Measurement of Melt Pool Characteristics in Selective Electron Beam Melting of Ti-6Al-4V", The International Journal of Advanced Manufacturing Technology, 88, 1309–1317, (2016).

[20] Mollamahmutoglu, M., Yilmaz, O., Unal, R., Gumus, B., Tan, E., "The effect of evaporation and recoil pressure on energy loss and melt pool profile in selective electron beam melting", The International Journal of Advanced Manufacturing Technology, (2022).

[21] Gu, H., Gong, H., Dilip, J.J.S, Pal, D., Hicks, A., Doak, H., Stucker, B., "Effects of powder variation on the microstructure and tensile strength of ti6al4v parts fabricated by selective laser melting", 25th annual international solid freeform fabrication symposium, (2014).

[22] Mollamahmutoğlu, M., Yılmaz, O., "Volumetric heat source model for laser-based powder bed fusion process in additive manufacturing", Thermal Science and Engineering Progress, 25, 101021, (2021).

[23] Yıldız, A. K., Mollamahmutoğlu, M., Dogan, E., Yılmaz, O., "A numerical investigation of the effect of support thickness and void ratio on thermal behavior and possible martensite decomposition in laser powder-bed fusion process", Journal of Additive Manufacturing Technologies, 1(2), 549, (2021).

[24] Salsi, E., Chiumenti, M., Cervera, M., "Modeling of microstructure evolution of Ti6Al4V for additive manufacturing", Metals, 8, 633, (2018).

[25] Ahmed, T., Rack, H.J., "Phase transformations during cooling in α+β titanium alloys", Materials Science and Engineering: A, 243, 206–211, (1998).

[26] Gan, M.X., Wong, C.H., "Practical support structures for selective laser melting," Journal of Materials Processing Technology, 238, 474-484, ISSN 0924-0136, (2016).